Evaluation of cell affinity on poly(L-lactide) and poly(ε-caprolactone) blends and on PLLA-*b*-PCL diblock copolymer surfaces

Diana Ajami-Henriquez,[1] Mónica Rodríguez,[1] Marcos Sabino,[2] R. Verónica Castillo,[3] Alejandro J. Müller,[3] Adriana Boschetti-de-Fierro,[4] Clarissa Abetz,[4] Volker Abetz,[4] Philippe Dubois[5]

[1]*Departamento de Biología Celular, Universidad Simón Bolívar, Apartado 89000, Caracas, Venezuela*
[2]*Departamento de Química, Universidad Simón Bolívar, Apartado 89000, Caracas, Venezuela*
[3]*Grupo de Polímeros USB, Departamento de Ciencia de los Materiales, Universidad Simón Bolívar, Apartado 89000, Caracas, Venezuela*
[4]*Institute of Polymer Research, GKSS Research Centre Geesthacht GmbH, 21502 Geesthacht, Germany*
[5]*Laboratory of Polymeric and Composite Materials (LPCM), University of Mons-Hainaut, Place du Parc 20, 7000 Mons, Belgium*

Received 30 March 2007; revised 18 May 2007; accepted 16 July 2007
Published online 9 January 2008 in Wiley InterScience (www.interscience.wiley.com). DOI: 10.1002/jbm.a.31796

Abstract: An evaluation of cell proliferation and adhesion on biocompatible film supports was performed. A series of films were compression molded from commercially available poly (L-lactide), PLLA, and poly(ε-caprolactone), PCL, and from their melt mixed blends (PLLA/PCL blends). These were compared with compression molded films of PLLA-*b*-PCL model diblock copolymers. The samples were analyzed by differential scanning calorimetry (DSC), contact angle measurements, and scanning force microscopy (SFM). Cell adhesion and proliferation were performed with monkey derived fibroblasts (VERO) and with osteoblastic cells obtained either enzymatically or from explants cultures of Sprague–Dawley rat calvaria. Migration studies were performed with bone explants of the same origin. The results obtained indicate that although all materials tested were suitable for the support of cellular growth, a PLLA-*b*-PCL diblock copolymer sample with 93% PLLA was significantly more efficient. This sample exhibited a unique surface morphology with long range ordered domains (of the order of 2–3 μm) of edge-on PLLA lamellae that can promote "cell contact guidance." The influence of other factors such as chemical composition, degree of crystallinity, and surface roughness did not play a major role in determining cell preference toward a specific surface for the materials employed in this work. © 2008 Wiley Periodicals, Inc. J Biomed Mater Res 87A: 405–417, 2008

Key words: poly(L-lactide); poly(ε-caprolactone); diblock copolymers; cell adhesion and proliferation; bone explants

INTRODUCTION

The use of polymers in medicine has increased drastically over the last decades, and extensive research has illustrated their importance as implant devices not only in bone repair, but as useful scaffolds for organ and tissue regeneration.[1–3] Biodegradable polymers are ideal candidates for application in regeneration systems.[4] In the first place, they are readily accessible commercially and present remarkable mechanical ability to be shaped, secondly polymeric matrices can be selectively modified to promote growth and compatibility with the tissue of interest and finally their controlled degradation makes removal of the polymeric implant unnecessary.[1,5]

In the development of new biomaterials,[6,7] the initial interaction of cells with material substrates is of fundamental importance and contributes to the clinical success of implants.[8] The functional activity of cells in contact with the biomaterial is a consequence of how cells are capable of sensing, interpret, and integrate extra cellular signals. Therefore, the chemical and physical properties of the surface of a biomaterial, such as chemical structure, topography, electric charge, surface energy, and wettability are crucial parameters to be considered in the interaction

Correspondence to: A. J. Müller; e-mail: amuller@usb.ve or D. Ajami-Henriquez; e-mail: dajami@usb.ve

Contract grant sponsor: FONACIT; contract grant number: S1-2001000742

between the material and the biological environment and therefore in the regulation of cell behavior.[4,9,10] Topographic scale (at the micron or nano level) is an important biomimic regulator of cell behavior. Cells *in vivo* exist in topographic interfaces closer to the nanometer scale than to the micrometer scale, for example, the cross-striation pattern every 67 nm of type I collagen, the 10-nm thick fibrils and 20 nm pores of rat kidney membrane, and the 20–200-nm felt-like topography of human cornea basement membrane.[11]

One such group of polymers that has gained considerable attention in the field of orthopedic surgery, as potential scaffolds for repairing bone defects, are the biodegradable aliphatic polyesters such as poly(L-lactic acid) (PLLA) and poly(ε-caprolactone) (PCL).[1,12,13] Both polymers have been reported to induce minimal inflammatory response and favorable biocompatibility characteristics. In the last few years, many researches have focused on improving their performance as biomaterials by selectively modifying them to promote hydrophilicity and cell adhesion. This has been performed by introducing functional groups onto the polymer surface or inducing morphological or topographic modifications.[14]

A combination of PCL and PLLA in a single material could be employed to tailor materials properties such as bio-absorption time or mechanical properties. If high molecular weight materials are employed, PCL/PLLA blends are known to be immiscible and a dispersion of one material on the other can be produced by for instance melt blending.[15] Another way of combining these two polymers is by producing copolymers. If block copolymers are produced, a better control on the composition and morphology can be obtained besides avoiding macro-phase segregation. The morphology and structure of block copolymers has been the subject of several recent reviews.[16–18]

In this article, a series of polymer films were prepared with PLLA/PCL blends and with PLLA-*b*-PCL diblock copolymers with the objective of producing diverse surface morphologies which could have affinity with different types of cells. In order to evaluate cell adhesion and proliferation on these biomaterials, a fibroblastic cell line (VERO cells) and a primary culture of osteoblasts obtained from rat calvaria were employed.

MATERIALS AND METHODS

Materials

In this work, we have employed neat PLLA and PCL homopolymers of two different molecular weights and blends and block copolymers that are described in the following paragraphs.

Synthesis and characterization of diblock copolymers

The block copolymers were synthesized by controlled/"living" sequential block copolymerization as initiated by aluminum trialkoxides in toluene solutions as previously described.[19] The diblock copolymer nomenclature used denotes the PLLA block as L and the PCL block as C, subscripts indicate the approximate composition in weight % and superscripts the approximate number average molecular weight in kg/mol. Two homopolymers of comparable molecular weights were prepared for comparison purposes, that is, PCL^{29} and $PLLA^{24}$ (with number average molecular weights of 29 kg/mol and 24 kg/mol, respectively). Compositions studied were $L_{93}{}^{16}C_{07}{}^{2}$, $L_{81}{}^{17}C_{19}{}^{4}$, and $L_{60}{}^{12}C_{40}{}^{9}$. Recent works have reported the morphology, structure and crystallization behavior of the PLLA-*b*-PCL diblock copolymer samples employed here.[20,21]

Preparation of blends

In the case of melt-mixed blends, two commercial materials were employed. A PCL manufactured by Union Carbide with an M_n = 120 kg/mol and a PLLA supplied by Purac Biochem with an M_n = 86 kg/mol. They will be denoted as: PCL^{120} and $PLLA^{86}$. Blends were prepared by extrusion in an ATLAS Laboratory Mixing Extruder at compositions equivalent to those of the copolymers at 180°C and 30 rpm (PCL was extruded at 160°C). Blends compositions of PLLA/PCL 93/07, 81/19, and 56/44 were evaluated and compared with their respective homopolymers. It is important to note that blends and block copolymers differ in the molecular weight of the PCL and PLLA components. This is why we have employed also neat homopolymers of different molecular weights. Therefore, comparisons will always be made with the corresponding equivalent molecular weight homopolymers. In the case of PLLA this is particularly important, since $PLLA^{24}$ can readily crystallize upon cooling while $PLLA^{86}$ can not in view of the differences in crystallization kinetics induced by the differences in molecular weights.

Preparation of films

All the samples (blends and copolymers) were compression molded at 190°C for 3 min (the PCLs were molded at 120°C) employing mirror polished stainless steel mold plates with an inner frame. Between the steel mold plates, Kapton films were placed in order to avoid demolding problems. The samples were cooled by placing them in the lab bench at room temperature, that is, air convection. Films of 0.1-mm thick were obtained and employed without any further treatment.

Contact angle assay

Films of 0.1 mm were analyzed by the sessile drop method using a contact angle meter (OCA15+) with high-performance image processing system from Data Physics Instruments. The liquids used were H_2O and CH_2I_2 (both HPLC grade) and were added by a motor driven syringe at room temperature. Three samples of each material were used and five measurements were carried out for each sample. The presented results were calculated using the final average values. The polarity of the surface as well as the surface tension was calculated by the Owens–Wendt equation.[22]

Thermal analysis

A Perkin-Elmer DSC-7 differential scanning calorimeter was employed for calorimetric assays. Samples were encapsulated in aluminum pans (mass was ~5 mg in all cases). The calibration was performed with Indium and Hexatriacontane and all tests were run employing ultra pure nitrogen as purge gas. Standard DSC heating scans were performed at 10°C/min, from 25 to 200°C.

Cell Culture Methodology

Fibroblasts cell line

Monkey derived Fibroblast Cell Line (VERO) were grown in Dulbeco's Modified Eagles Media (MEM), supplemented with 10% fetal bovine serum (FBS) (GIBCO Laboratories), 1% penicillin/streptomycin, and 1% fungyson (supplied by SIGMA). The cells were maintained in a gas-jacket incubator at 37°C in a controlled humidified atmosphere at 5% CO_2/95% air. Confluent cell cultures were sub-cultured every 4 days by dissociating cells with 0.05% trypsin (GIBCO Laboratories) in phosphate buffered saline (PBS).

Isolation and culture of osteoblastic cells

Osteoblastic cells were obtained either enzymatically or from explants cultures of Sprague Dawley rat calvaria.

Enzymatic isolation

Osteoblastic cells were isolated from newborn (2 days) rat calvaria by the method of Pei and coworkers[23] with minor modifications. The calvarias were removed of skin, soft connective tissue and periosteum, digested sequentially in a 0.125% trypsin, 0.1% collagenase, EDTA 0.5*M* (ethylenediaminetetraacetic acid) (supplied by SIGMA) solution in PBS at 37°C first for 10 min followed by four digestions of 20 min. Rat calvaria cells, obtained from the third digestion (20 min), were pooled and plated in a Petri tissue culture dish (Costar, USA) with culture medium (MEM) supplemented with 10% FBS 1% penicillin/streptomycin 1% fungizon (supplied by SIGMA) and 50 μg ascorbic Acid (supplied by SIGMA) in a controlled atmosphere.

Explants culture

Calvarias were treated as described previously and cell migration from bone explants was measured as described previously.[24] Briefly, extracted calvaria were cut into pieces of approximately (2×2) mm^2. Bone pieces were placed on the bottom of a 96 wells tissue culture dish in which the different test substrates were previously placed. The initial incubation was done in the absence of media in order to facilitate the attachment of the bone pieces to the different polymers. After 45-min incubation, culture media was added. Cultures were incubated in a controlled atmosphere.

Adhesion assay

The different polymers films were cut into small disks with the aid of a cork borer, sterilized by UV and placed on the bottom of a 96 cell culture plate (Costar, USA). Confluent cultures of fibroblasts or osteoblastic cells were trypsinized and collected by centrifugation at 750 rpm for 3 min, suspended in cell culture medium (with 50 μg/mL ascorbic acid in the case of osteoblastic cell cultures) to a concentration of 5×10^3 cells per well, in a total volume of 2 mL. After seeding, the cultures were incubated for 6 h at 37°C in 5% CO_2/95% air. At the end of this period, wells were washed twice with PBS to remove non attached cells. The number of viable cells attached on the different polymers was evaluated by the MTT assay[10] (3-(4,5-dimethylthiazol-2-yl)-2,5-diphenyltetrazolium bromide assay). The obtained results are reported as optical density (OD). In this test, MTT-formazan production was used to evaluate succinic dehydrogenase enzyme activity in the mitochondria of cells, an indicative of the presence of viable cells.

Proliferation assay

Fibroblast and osteoblastic cell suspensions, containing 5×10^5 cell/well were seeded on the experimental substrates as described previously for the cell adhesion assay and incubated at 37°C in 5% CO_2/95% air for 6 and 92 h. At the end of the incubation period, non adherent cells were removed by washing with PBS. The number of cells attached was measured as described previously by the MTT assay.

Outgrowth assay

Calvaria explants were located in contact of the different polymers to be studied as described previously. Cell outgrowth from bone explants and morphology were assessed by optical and scanning electron microscopy (SEM).

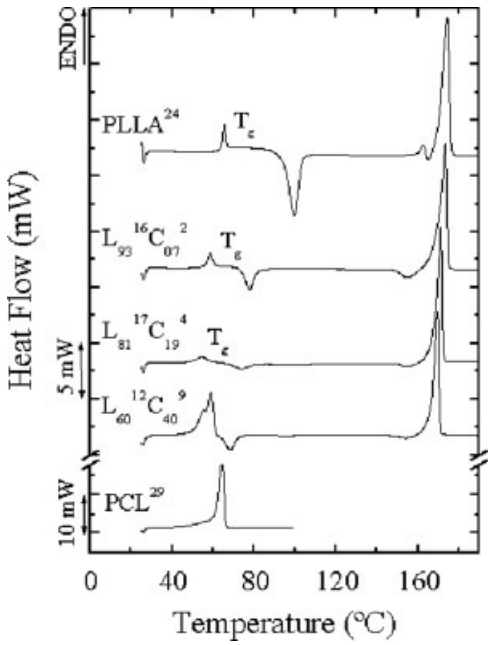

Figure 1. First DSC heating scans at 10°C/min for PLLA-*b*-PCL diblock copolymers compression molded films.

Morphology assays

Optical microscopy

Osteoblastic cells and bone explants seeded on the different films were washed twice with PBS and films were stained with May Grunwald-Giemsa stain as previously described.[10,25]

Scanning electron microscopy

Bone explants were fixed *in situ* with a 2.5% solution of gluteraldehyde for 45 min at 4°C and rinsed twice with PBS for 15 min at 4°C. Post fixation was made in 1% OsO_4 in Sabatini buffer at pH 7.4 for 60 min at 4°C. After this period, the samples were washed twice with the same buffer for 5 min followed by dehydration in a graded series of methyl ketone (30, 50, 70, 90, 95, and 100%) for 10 min in each solution at 4°C. Following the fixation and dehydration process, the samples were introduced in a critical point drying for 30 min. Finally, the specimens were mounted and coated with gold palladium and examined on an S-500 Hitachi Electron Microscope operated at 5 kV.

Scanning force microscopy

Scanning force microscopy (SFM) images were taken with a Veeco Multimode in the tapping mode. The surfaces of the compression molded films were observed without any further preparation. The images were taken on a "Digital Instruments" MultiMode™ AFM with a NanoScope IV controller. The equipment was used in tapping mode at ambient conditions. Commercial silicon TM AFM tips (model MPP 12100) with a free resonance frequency of 100–200 kHz and spring constant of 2.5–10 N/m were employed.

Statistical analysis

Multiple samples were collected in each measurement ($n = 3$) and expressed as mean ± standard deviations (SD). Single factor analysis of variance (ANOVA) method was used to assess the statistical significance of the result. p values less than 0.01 were considered significant and were denoted by *.

RESULTS AND DISCUSSION

Thermal characterization of blends and diblock copolymers

DSC first heating scans of molded films of block copolymers and homopolymers are shown in Figure 1 while Table I lists the observable transition enthalpies

TABLE I
Thermal Properties Obtained from DSC Scans Presented in Figures 1 and 2 for the Blends, Copolymers, and Homopolymers

PLLA/PCL (blends) Or $L_x^yC_x^y$ (Copolymers)	PLLA						PCL		
	T_g (°C)	T_c (°C)	T_m (°C)	ΔH_c (J/g)	ΔH_m (J/g)	X_c (%)	T_m (°C)	ΔH_m (J/g)	X_c (%)
PLLA[86]	59.7	114.4	159.4/164.7	36	38	2	–	–	–
93/07	–[a]	108.5	157.5/164.2	32	34	2	59.8	–	–
81/19	–[a]	107.0	157.2/163.8	33	36	3	59.3	52	39
56/44	–[a]	106.9	156.7/163.5	35	44	10	60.2	59	43
PCL[120]	–	–	–	–	–	–	56.4	61	45
PLLA[24]	62.9	99.7/165.0	162.5/174.4	43	65	23	–	–	–
$L_{93}{}^{16}C_{07}{}^{2}$	53.8	77.7/154.9	173.4	21	65	47	–	–	–
$L_{81}{}^{17}C_{19}{}^{4}$	46.0	73.7/101.0 131.3/154.3	171.2	10	58	51	54.2	–	–
$L_{60}{}^{12}C_{40}{}^{9}$	–[a]	68.4/153.7	169.5	15/7	72	53	58.9	67	49
PCL[29]	–	–	–	–	–	–	64.2	88	65

[a]These values were not clearly detected because of an overlap with the melting endotherm corresponding to the PCL phase.

and temperatures. The peak melting temperature of PLLA blocks shows a small decrease upon increasing PCL content within the block copolymers and with respect to neat PLLA[24]. Glass transitions of PLLA blocks can also be seen in Figure 1, where they can easily be recognized as an endothermic step with a small enthalpic relaxation peak (which can, in some cases, overlap with PCL melting endotherms), and they decreased as the content of PCL increased, indicating a degree of miscibility between the components. According to previous works,[20,21] PLLA-*b*-PCL block copolymers are either mixed in the melt or weakly segregated (i.e., they mostly crystallize from a mixed melt except at compositions close to 50–50 when they can form well organized melt structures which are later destroyed or modified by the crystallization of each block). Partial miscibility can induce a diluent effect of the PCL block over the PLLA block, depressing both T_c and T_m of the PLLA block.

Cold crystallizations of PLLA block can be seen for all compositions in Figure 1. The degree of crystallinity of the PLLA block in the molded films was calculated by subtracting the heat of cold crystallization from the heat of fusion. These values are shown in Table I, and are calculated neglecting reorganization phenomena that could not be registered by DSC. Crystallization kinetics of PCL is also significantly impaired due to the covalently bonded PLLA block which crystallizes first during cooling. Because of this, PCL blocks remain virtually amorphous in the molded films when present in 7 and 19%.

Figure 2 presents DSC first heating scans for the compression molded blend films. It is remarkable how the blends exhibit two melting temperatures that are very close to those obtained for the parent homopolymers (a higher T_m for PCL[29] was observed as compared with the PCL[120] phase in the blends due to differences in molding conditions as will be explained later), a clear sign of immiscibility. It should be noted that the T_g of PLLA[86] is located around 60°C. However, in the blends the T_g is overlapped with the melting of the PCL[120] phase and therefore it cannot be seen, so it is difficult to use PLLA[86] T_g values as a miscibility criterion. The T_g of the PCL[120] is located at −65°C, outside the temperature range of the cooling device employed with our DSC. However, the immiscibility of these components with a high molecular weight has been reported in the literature[6,15] and as stated above, the invariance of T_m with composition is also a clear sign of immiscibility. The degree of crystallinity was calculated and presented in Table I.

Remarkable differences in thermal behavior can be seen for the two PLLA homopolymers employed here. PLLA[86] has lower T_g and T_m values (see Table I) than PLLA[24] suggesting that the stereoregularity in PLLA[86] is not as high as in PLLA[24] as far as

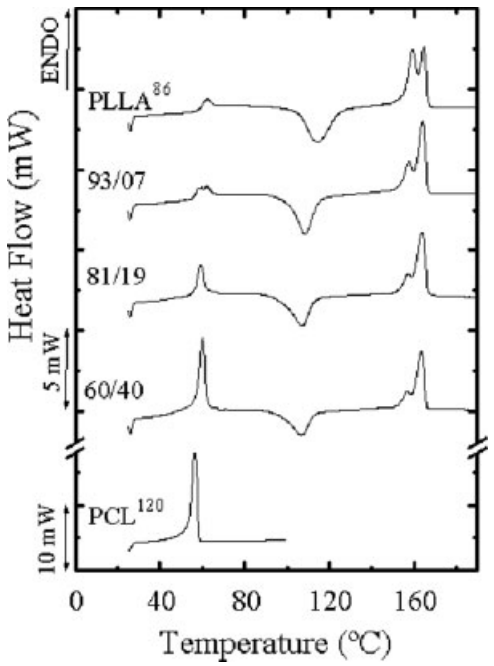

Figure 2. First DSC heating scans at 10°C/min for PLLA[86]/PCL[120] blends compression molded films.

the content of the L stereoisomer is concerned (a fraction of D isomer is probably present in the sample). This can also explain why PLLA[86] has a much lower crystallization rate than PLLA[24]. The crystallization kinetics of PLLA is also highly dependent on its molecular weight and decreases sharply as the molecular weight increases. Therefore, PLLA[86] remains amorphous when it is cooled at the rate of 10°C/min or higher. The molded films of PLLA[86] were cooled by air convection and crystallize only 2% during its preparation (see Table I).

In the case of the PCL[120] phase within the PLLA/PCL blends, the degree of crystallinity does not vary significantly until the PCL content is reduced to 19%. For such low PCL contents and lower, a fine droplet dispersion of PCL[120] within PLLA[86] is obtained and fractionated crystallization may occur.[17,26] However, an unexpected increment in the melting temperature of PCL[120] in the blends with respect to PCL[120] homopolymer is also observed. Higher melting temperatures are associated to thicker lamellar crystals. The blends were molded at 190°C (see Experimental section) and the PCL[120] homopolymer was molded at 120°C. This difference in the molded temperature causes different crystallization conditions. Higher molded temperature implies slower crystallization rate therefore thicker lamellae.

Contact angle measurements

The surface hydrophilicity of various PLLA/PCL blends and diblock copolymers was determined by

TABLE II
Water Contact Angle measurements and Surface Energy for Homopolymers, PLLA/PCL blends, and Diblock Copolymers

Surface	θ_{H_2O} (°)	$\theta_{CH_2I_2}$ (°)	γ (mN/m^2)
PCL[29]	82.5 ± 6.6	48.0 ± 8.5	33.4
PLLA[24]	80.9 ± 2.3	44.6 ± 7.9	36.8
PLLA/PCL 56/44	85.9 ± 6.1	36.0 ± 5.3	38.7
$L_{60}{}^{12}C_{40}{}^{9}$	86.5 ± 3.4	36.5 ± 6.7	39.5
PLLA/PCL 93/07	81.1 ± 1.9	44.9 ± 1.4	37.1
$L_{93}{}^{16}C_{07}{}^{2}$	83.5 ± 2.0	35.2 ± 4.0	41.0

contact angle measurements and the data are presented in Table II. Both PLLA[24] and PCL[29] are hydrophobic polymers as shown by their large contact angles in water. For all samples tested, no significant differences were observed in the measured contact angles when water was used for evaluating the interaction with the biomaterial surface suggesting similar hydrophobic behavior as was expected due to the closer values of θ of the homopolymers. Similar results were also observed with methylene iodide. Roughness surface can also affect contact angle measurements, that is textured surface has generally lower values than flat films.[11] The total surface energy (γ) was calculated by the Owens–Wendt equation.[22] The results obtained indicate that blends and copolymers present slightly higher surface energy values than those obtained for the homopolymers. More specifically, the $L_{93}{}^{16}C_{07}{}^{2}$ copolymer exhibits the highest value in surface energy (although the difference with the other samples is not very large). This enhanced surface energy can stem from the surface characteristics of the film and may induce a slightly larger bio-interaction and biocompatibility[27] on this particular sample as compared with the others.

Determination of polymer surface topography with SFM

Figure 3 shows representative surface morphologies visualized by SFM height and phase images of selected samples at two magnifications. The height image reflects the sample topography, since the samples were compression molded, the images yield information regarding the smoothness of the film and the surface morphology.[28] The roughness of the sample and its height variation limit the amount of information contained in the topography images presented in Figure 3.

The phase image of SFM is generated based on the viscoelastic differences among the phases or materials present on the surface, and can be used to qualitatively differentiate phases on the surfaces of heterogeneous samples.[29,30] Although artifacts sometimes are present in this kind of technique because of its high sensitive to scanning parameters, the results presented below were reproducible.

In the representation shown here, the material with the highest modulus will be depicted in a lighter color than the material with the lowest color. In samples with crystalline and amorphous phases, crystallites or crystalline lamellae appear brighter (or whiter) while the amorphous soft phases appear darker.

The PLLA[24] in Figure 3 shows a typical lamellar morphology that corresponds to a portion of a spherulite. Spherulites were previously observed by polarized light optical microscopy of the same samples.[20,21] The granular substructure of the lamellae that can be observed in the images is also a common feature of polymer crystallization and has recently been connected with new theories of polymer nucleation and growth.[31]

In the case of $L_{93}{}^{16}C_{07}{}^{2}$ [Fig. 3(c–d), phase images] a similar morphology to that of PLLA[24] can be seen. However, in this case, the sample can crystallize up to almost twice as much as PLLA[24] (see Table I), and only the PLLA block undergoes crystallization. Therefore, we have a surface with a higher crystalline content and with crystalline lamellae that are substantially longer and appeared to have some longer range orientation than those within PLLA[24]. Having large portions of edge-on lamellae oriented on the surface in a scale of 2–3 μm makes this material unique with respect to all the others examined here that always contained much shorter lamellae. The reason why $L_{93}{}^{16}C_{07}{}^{2}$ exhibits such long range orientation on the surface of the prepared films, as compared to the rest of the materials employed here, is not clear.

One major difference between the blends and the block copolymers compared here is that the PLLA[86] used for the blends has a substantially higher molecular weight (and different stereoregularity, that is, a lower L isomer content) as compared to PLLA[24]. As mentioned previously, this is the reason why, PLLA[86] could only crystallize 2% when the samples were prepared and the same amount when it was blended with PCL in a 93/07 ratio. Therefore, it is not surprising that the morphology of the surface of the 93/07 blend shown in Figure 3(e–f) (phase images) was mainly featureless, indicating a very low viscoelastic contrast due to the low crystalline content. The image shown in Figure 3(f) (phase image) pictures what appears to be some lamellar bundles that were only visible once the surface was subjected to hard tapping force. This indicates that the lamellae are covered with a superficial amorphous layer. A general fea-

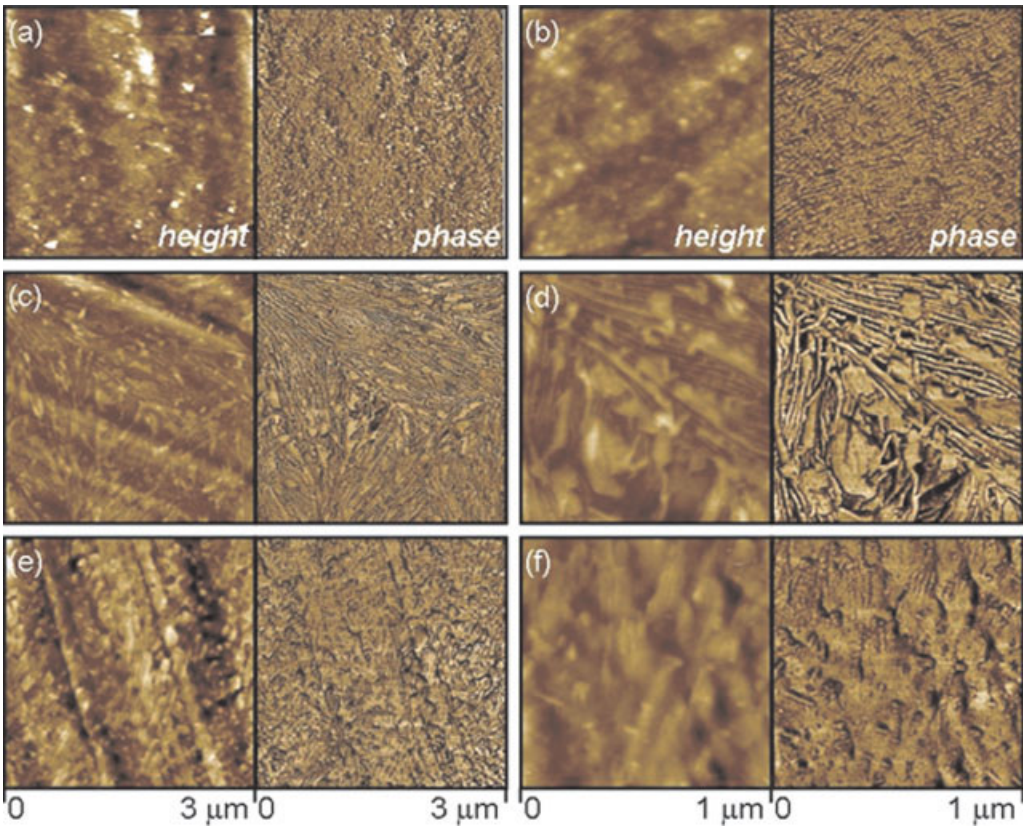

Figure 3. SFM height (left) and phase (right) images of selected PLLA-*b*-PCL copolymers. (a) 3 μm images and (b) 1 μm images of PLLA[24] homopolymer, (c) 3 μm images and (d) 1 μm images of $L_{93}{}^{16}C_{07}{}^{2}$ block copolymer, (e) 3 μm images and (f) 1 μm images of 93/07 PLLA/PCL blend. Z_{max} = 50 nm in all images, except in (d), where Z_{max} = 40 nm. [Color figure can be viewed in the online issue, which is available at www.interscience.wiley.com.]

ture of the blend samples was to have lower surface degrees of crystallinity as compared with the block copolymer samples employed here.

With the purpose of quantifying the morphology of the surface of the films employed for cell adhesion and proliferation, the determination of the mean lamellar size and surface roughness was performed employing the Nanoscope 6 software. In Figure 4 (left), a blue rectangle denotes one section of the picture initially employed for quantitative analy-

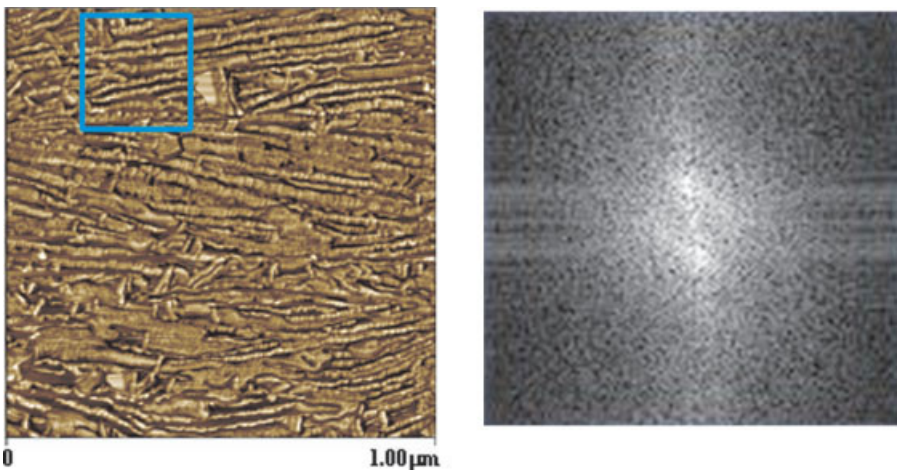

Figure 4. Left SFM phase image of $L_{93}{}^{16}C_{07}{}^{2}$ block copolymer. The blue rectangle denotes the section of the picture employed for quantitative analysis. Right: Image corresponding to the fast Fourier transform (FFT) of the SFM picture in the blue rectangle in the left side. [Color figure can be viewed in the online issue, which is available at www.interscience.wiley.com.]

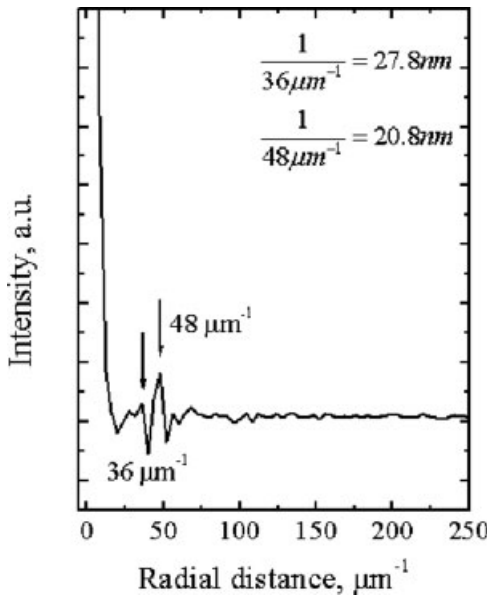

Figure 5. Linear integration (from the center to the top) to the fast Fourier transform (FFT) of the SFM picture showed in Figure 4.

sis corresponding to the phase image of $L_{93}{}^{16}C_{07}{}^{2}$. Figure 4 (right) shows an image corresponding to the Fast Fourier Transform (FFT) of the SFM phase image (blue rectangle in Fig. 4). If this image is integrated linearly from the center to the top, that is, through the reflection of highest intensity, Figure 5 is obtained and the maximum of the radial integration should correspond to the average reciprocal repeating long period. The long period is the average repeating distance from the center of one lamella to the center of the next one and it is proportional to the mean lamellar thickness of the portion of the sample examined (as long as the interlamellar amorphous region has a constant packing density).

Figure 5 shows two main maxima which have been noted with arrows and correspond to 36 and 48 μm^{-1}. They are equivalent to mean long periods of 27.8 or 20.8 nm, respectively.

A second procedure to quantify the long periods and check for the validity of the FFT analysis is shown in Figure 6 and corresponds to the analysis of a slice of the height images presented in Figure 3.

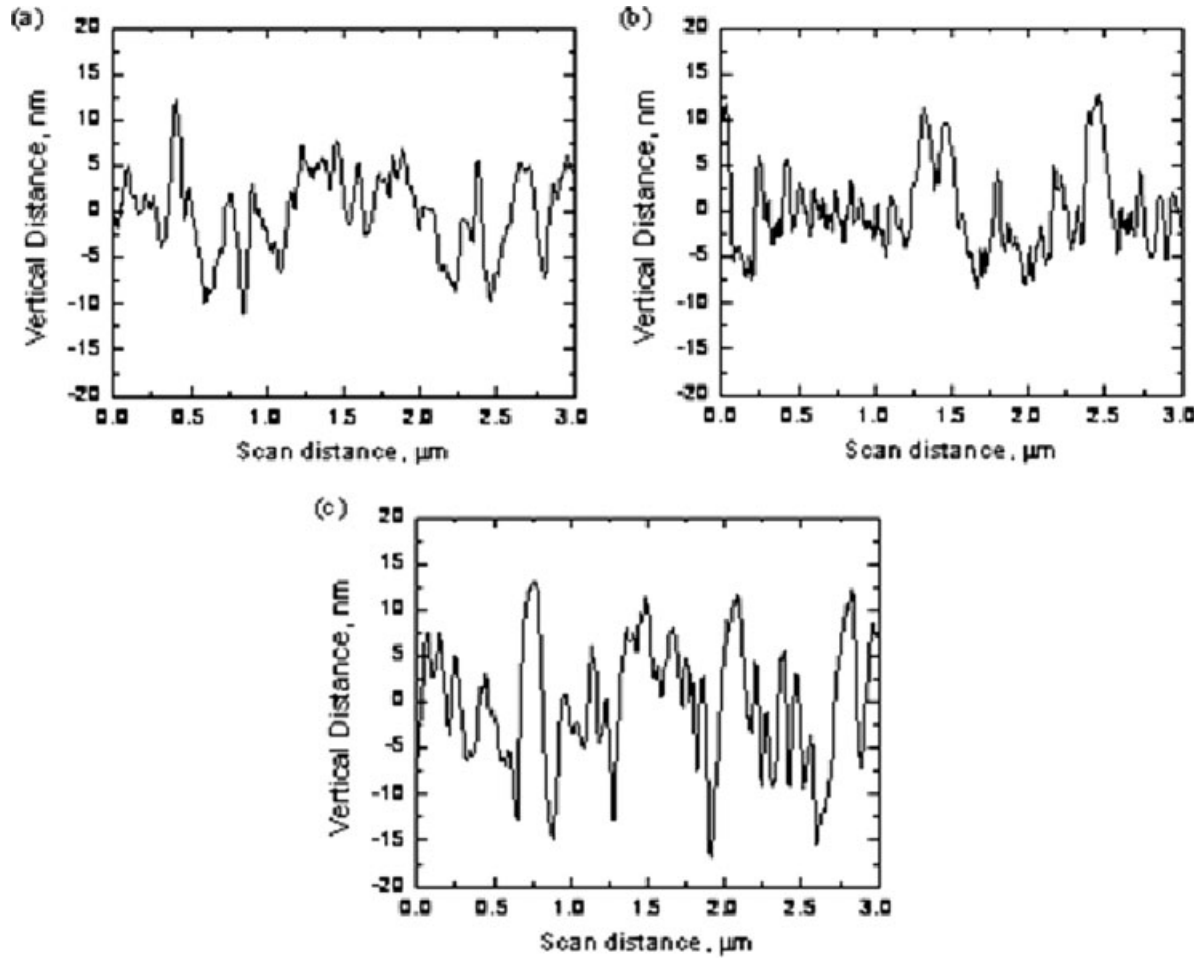

Figure 6. Vertical slices of the 3 μm SFM height images in Figure 3. (a) $PLLA^{24}$ homopolymer, (b) $L_{93}{}^{16}C_{07}{}^{2}$ block copolymer, and (c) 93/07 PLLA/PCL blend.

TABLE III
Surface Roughness Parameters and Lamellar Thickness Calculated from the SFM Height and Phase Images for the Blends, Copolymers, and Homopolymers

	Roughness		Section Cut	FTT Integration
Surface	R_q (nm)	R_a (nm)	l (nm)	l (nm)
PLLA/PCL 93/07	4.63	3.66	22 ± 4	
PLLA/PCL 56/44	0.43	0.34		
PLLA[24]	4.57	3.63	20 ± 3	
$L_{93}{}^{16}C_{07}{}^{2}$	2.75	2.3	27 ± 7	27.8 and 20.8
$L_{60}{}^{12}C_{40}{}^{9}$	6.23	4.75	21 ± 4	38.5 and 29.4

The observed profile is therefore based on the differences in height in between the crystalline and amorphous portions of the surface. In the case of the sample $L_{93}{}^{16}C_{07}{}^{2}$, the mean distance between peaks (from 20 measurements) represents the long period and yields a value of 27 ± 7 nm. This value represents a good match with those obtained by FFT analysis. This procedure was repeated for several samples including $L_{60}{}^{12}C_{40}{}^{9}$ and the same result was observed for PLLA[24] and for the block copolymers, the lamellar long period was always in between 20 and 30 nm (see Table III). This is probably caused by the constant cooling conditions employed to mould the films. We can therefore rule out the lamellar thickness as a variable in determining any preference for cells to adhere or proliferate on a particular block copolymer sample or on PLLA[24].

Two types of roughness measurements were performed. First the arithmetic average of the absolute values of the surface height deviations measured from the mean plane (R_a) was calculated as:

$$R_a = \frac{1}{N}\sum_{j=1}^{N} |Z_j| \quad (1)$$

Then the root mean square average of height deviations taken from the mean image data plane (R_q) was calculated as:

$$R_q = \sqrt{\frac{\sum Z_i^2}{N}} \quad (2)$$

and the values obtained were R_a = 2.3 nm and R_q = 2.75 nm for the sample $L_{93}{}^{16}C_{07}{}^{2}$ (see Table III).

The same type of quantitative analysis was performed to the images shown in Figure 7 corresponding to the surface of sample $L_{60}{}^{12}C_{40}{}^{9}$. In this case, this block copolymer also shows a series of edge-on lamellae at the surface, although much shorter in length than those observed in the surface of $L_{93}{}^{16}C_{07}{}^{2}$ [compare with Fig. 3(c,d)]. The values of roughness obtained for $L_{60}{}^{12}C_{40}{}^{9}$ were higher (i.e., R_a = 6.23 nm and R_q = 4.75 nm, see Table III).

As Table III shows, the surface roughness was similar for almost all samples (i.e., it fluctuated in between 3 and 6 nm) except for the blend 56/44 whose surface was particularly smooth.

We can conclude from the AFM results that the copolymer $L_{93}{}^{16}C_{07}{}^{2}$ stands out amongst all samples examined here because it has long range order domains of edge-on surface lamellar regions. The roughness of the surface of this sample is comparable with others, therefore what makes it unique is its long range order on a 2-3 μm scale.

Cellular response

The *in vitro* cellular response to the different polymeric films was assessed in terms of initial adhesion, proliferation, morphology, and cell migration. Two types of cells were considered for this study: a monkey (VERO) immortalized cell line and primary rat calvaria osteoblasts.

Cell adhesion and proliferation

To study adhesion and proliferation on different films, cultured fibroblasts and osteoblasts were seeded on the different materials to be tested and cell adhesion was measured after a 6 h incubation period (see Experimental section). As can be observed in Figure 8 (light yellow bars) no significant differences were observed in the initial adhesion of both cell types seeded on the different polymeric substrates when compared with the value of OD obtained for the control tissue culture polystyrene (TCPS). The only exception to this was observed for the $L_{93}{}^{16}C_{07}{}^{2}$ diblock copolymer sample where a significant increase in initial adhesion ($p < 0.01$) was observed not only when compared with TCPS but with all the other films tested. The increased number of cells on the different polymer films at the end of a 96-h cultivation period demonstrated that proliferation occurred on all tested substrates (dark grey bars). However, for both cell types studied, a significant increase ($p < 0.01$) was again observed for the $L_{93}{}^{16}C_{07}{}^{2}$ copolymer, not only in relation to the values obtained for TCPS but also in relation to the homopolymers, and all other block copolymer and blend samples. It is interesting to note the slower proliferation observed on the PLLA/PCL 60/40 blend films in both cell types studied, despite an initial adhesion to the substrate. This blend exhibited macro-phase separation which was clearly observed during sample preparation by compression molding.

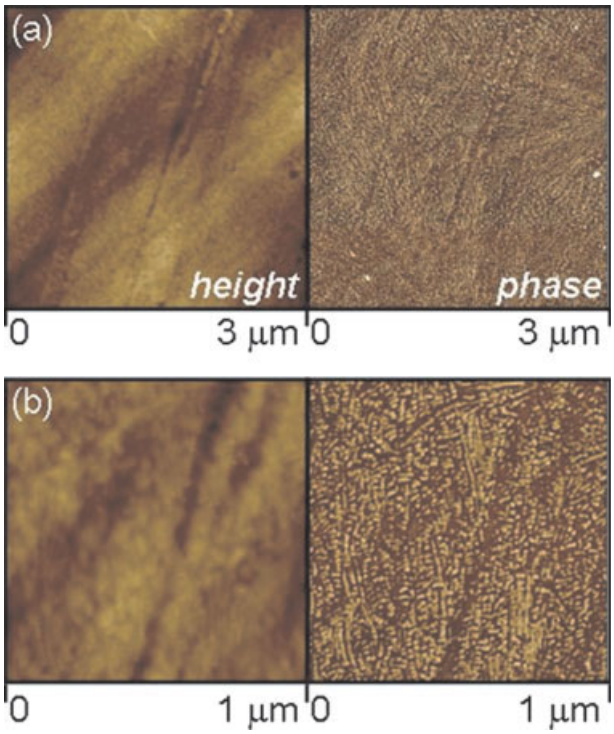

Figure 7. SFM height (left) and phase (right) images of $L_{60}{}^{12}C_{40}{}^{9}$ diblock copolymer sample. (a) 3 μm images, Z_{max} = 60 nm, (b) 1 μm images, Z_{max} = 40 nm. [Color figure can be viewed in the online issue, which is available at www.interscience.wiley.com.]

Osteoblast cell morphology

When evaluating cellular behavior on a biomaterial, cell morphology is a helpful indicator of biocompatibility. Rat calvaria osteoblasts were grown on the different films and stained with Giemsa-Maygrunwald at 7 days of subculture. Figure 9 is representative of the typical cell morphology observed in all polymeric films by optical microscopy. Cells were largely polygonal, with extended fillopodia and exhibited an organized monolayer of interacting cells. This cellular morphology observed is consistent with the results reported previously for osteoblasts grown on TCPS surfaces.[32–34]

Cell outgrowth from bone explants

To study the outgrowth of cells from explants on to the film surfaces, we used bone explants as described previously. As can be observed in Figure 10, SEM showed that after 1–2 weeks of incubation, cells started to migrate and proliferate from the borders of the explant. However, significant differences were observed for the different polymeric substrates studied. Very few cells were observed proliferating and migrating from explants seeded on PCL[29] [Fig. 10(a)] when compared with PLLA[24] [Fig. 10(b)]. In the former, it was possible to observe a great amount of fibrillar material, but fewer cells [Fig. 10(a)].

The more significant differences were observed in the case of cells growing from the perimeter of bone explants seeded on the $L_{93}{}^{16}C_{07}{}^{2}$ copolymer, the cells had a very flattened appearance (results not shown) and migrated and proliferated aligned to the edge-on lamellae on the polymer surface [Fig. 3(c,d)] with a pattern quite similar to the "contact guidance" caused by "groove-ridge."[32,34] Contrary to these results, cells growing from the perimeter of bone explants seeded on PLLA[24] appeared to be less aligned and with a more rounded morphology. These results may

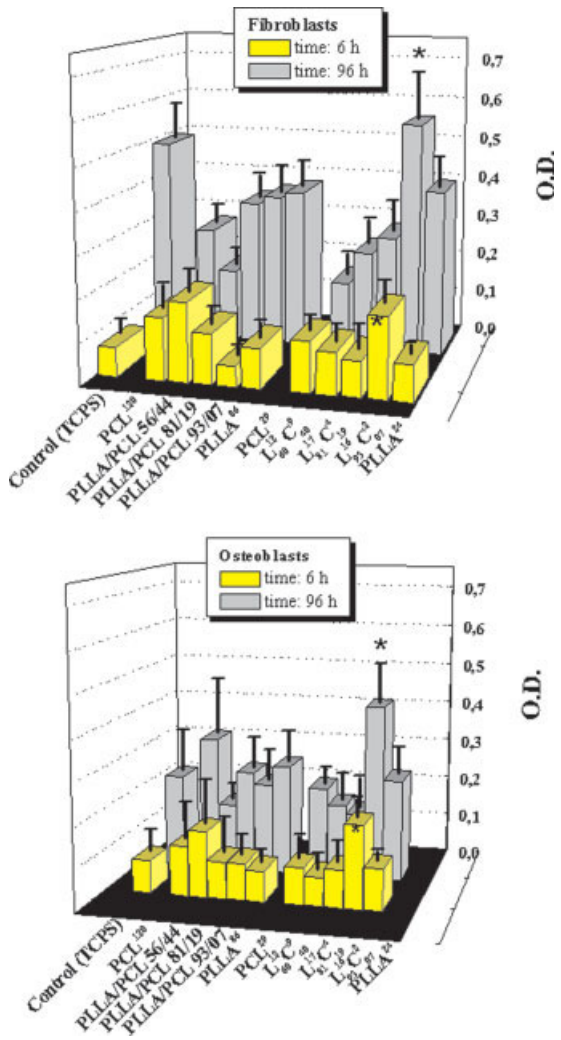

Figure 8. Adhesion and proliferation of fibroblastic VERO cells and osteoblasts grown on PLLA/PCL blends and diblock copolymers. Values given in the Figure represent the media of six different experiments and the error bars, the standard deviations. Light bars: adhesion measured at 6 h. Dark bars: proliferation at 96 h. (* denotes $p < 0.01$). [Color figure can be viewed in the online issue, which is available at www.interscience.wiley.com.]

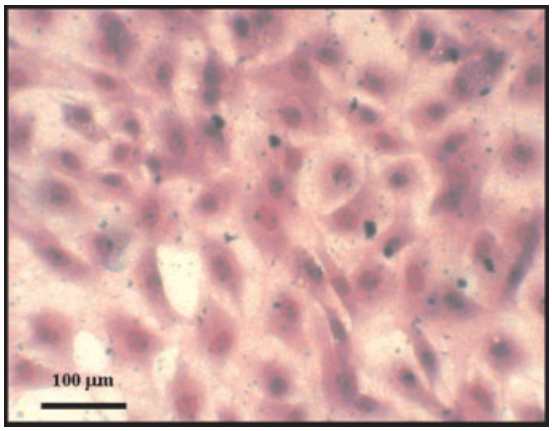

Figure 9. Morphology evaluation of rat calvaria osteoblasts on PLLA[24] films by optical microscopy: Cells were seeded on films and after 7 days of subculture cells were stained with Maygrunwald-Gimsa, magnification (×100). [Color figure can be viewed in the online issue, which is available at www.interscience.wiley.com.]

explain the increase of cell attachment efficiency observed for $L_{93}{}^{16}C_{07}{}^{2}$ copolymer. The results suggest that although all substrates tested were suitable for the support of cellular growth, $L_{93}{}^{16}C_{07}{}^{2}$ copolymer was significantly more efficient.

As widely reported, cells respond to different cues given by the biomaterial surface. Features such as wettability, chemistry, electric charge, surface energy, roughness, and rigidity are all known to act as extracellular stimulators and influence cell behavior.[10–12,33,35] Despite this knowledge, we are still far away from understanding the molecular basis and the relative importance of these features.

In our results, cell proliferation did not correlate with the measurements of wettability. Both PLLA and PCL are rather hydrophobic polymers and no significant differences were observed in contact angle measurements of the different copolymers or blends (Table III). The adhesion efficiency of the films tested and specifically of the $L_{93}{}^{14}C_{07}{}^{2}$ copolymer further corroborates the results reported by previous studies that indicate that wettability alone is not the only factor involved in cell behavior when addressing biomaterial efficiency.[11,33]

The differences in degree of crystallinity and chemical composition are also expected to influence cell response to the material surface. However, as the results of cell proliferation and adhesion demonstrate for the samples employed here, the cells do not show significantly different behavior towards neat PLLA or PCL regardless of their different molecular weights and structures. Also, even though there are important differences in crystallinity in between blends and copolymers, apparently for some compositions still the cells do not seem to recognize such differences. There seems to be a particular combination of chemical composition, surface topography and crystallinity in which cells preferentially adhere and proliferate.

Another factor that has important effects on the behavior of cells is surface morphology. Numerous reports have focused on how the morphology of a substrate surface influences the behavior of cells growing on such substrate *in vitro*.[5,32,33,35–37] In the last few years, the increasing use of micro and nanofabrication techniques has allowed the introduction of patterned surfaces such as grooves, ridges, pits, and islands on the polymer in order to study the effects of micro and nanometric topography on cellular behavior.[33,36,38]

Similarly to this work, Tang et al.[39] reported preferential cells adhesion in particular compositions of solution cast films of PLGA doped PCL with respective to homopolymers and other composition. This behavior was attributed to an specifically surface topography and hydrofilicity given by an hysteresis in contact angle measurements.

The introduction of a specific topography on biomaterial surfaces is of importance if we consider that cells *in vivo* live in an environment in which there are many nanostructures such as components of the

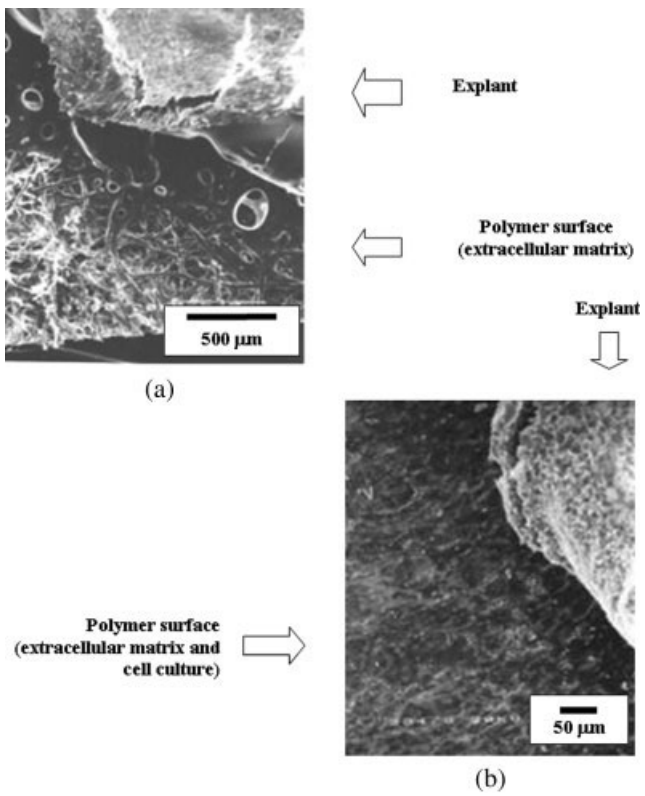

Figure 10. SEM micrographs of bone explants of rat calvaria on different polymer surfaces. Explants were seeded on films and observed by SEM at Day 14. Cell culture had a very flattened appearance and migrated and proliferated aligned to the surfaces: (a) PCL[29]; (b) PLLA[24].

extracellular matrix, for example, the striation pattern of collagen, as well as the surface of other cells in cell to cell contact.[32,40] Studies on the response of several cell types such as fibroblasts, osteoblasts, and epithelial cells have demonstrated that cells probably recognize surface features and respond to them by the formation of focal contacts,[40,41] reorganization of adhesion molecules such as integrins located within focal contacts[41,42] and of the cytoskeleton involved in signaling pathways important to control cell proliferation, migration, and differentiation.[41–43] Cells usually elongate in the direction of the groove and travel guided by the grooves in a phenomena known as "contact guidance" and the determinants of the alignment response are mainly the depth and width of the grooves.[38]

The SFM results performed in this study show a unique morphology in the case of $L_{93}{}^{16}C_{07}{}^{2}$, where samples presented a surface with a higher crystalline content and the crystalline lamellae were substantially longer and appeared to have some long range orientation. Having large portions of edge-on lamellae oriented on the surface in a scale of 2–3 μm makes $L_{93}{}^{16}C_{07}{}^{2}$ unique with respect to all the rest of the materials examined here, since they contained much shorter lamellae. These different characteristics can lead to the phenomena previously described as "cell contact guidance" and be responsible for the better performance of this polymer. Structural results of SEM, described previously, are in accordance with this conclusion (Fig. 10). It is also important to observe that SFM images of $L_{93}{}^{16}C_{07}{}^{2}$ (Fig. 3) showed a slightly rougher surface than other samples studied where amorphous layers lay on the surface. Surface roughness is another topographical feature to be implicated in cell adhesion and proliferation.[32,39,42] However, in the present case, it seems that the most important feature is the long range lamellar orientation on the film surface exhibited by the $L_{93}{}^{16}C_{07}{}^{2}$ diblock copolymer sample.

CONCLUSIONS

We can conclude from our results, first, that one sample stands out amongst the rest with respect to cell behavior. This is caused by its long range ordered domains of edge-on surface lamellar regions that permits a better alignment and better attachment efficiency to the polymer surface. This sample is the diblock copolymer $L_{93}{}^{16}C_{07}{}^{2}$. Second, this work illustrates the potential to fabricate unique surface morphologies with topographic features that significantly improve cell adhesion, migration, and proliferation by copolymerizing two hydrophobic biocompatible and biodegradable polymers such as PLLA and PCL.

References

1. Kronenthal RL, Oser Z, Martin E, editors. Polymers in Medicine and Surgery. Polym Sci Technol 8, New York: Plenum Press; 1975.
2. Safinia L, Mantalaris A, Bismarck A. Nondestructive technique for the characterization of the pore size distribution of soft porous constructs for tissue engineering. Langmuir 2006;22:3235–3242.
3. Na YH, He Y, Shuai X, Kikkawa Y, Doi Y, Inoue Y. Compatibilization effect of poly(ε-caprolactone)-*b*-poly(ethylene glycol) block copolymers and phase morphology analysis in immiscible poly(lactide)/poly(ε-caprolactone) blends. Biomacromolecules 2002;3:1179–1186.
4. Langer R, Vacanti J. Tissue Eng Sci 1993;260:920–926.
5. Battista S, Guarnieri D, Borselli C, Zeppetelli S, Borzacchiello A, Mayol L, Gerbasio D, Keene DR, Ambrosio L, Netti PA. The effect of matrix composition of 3D constructs on embryonic stem cell differentiation. Biomaterials 2005;26: 6194–6207.
6. Yang J-M, Chen H-L, You J-W, Hwang JC. Miscibility and crystallization of poly(L-lactide)/poly(ethylene glycol) and poly(L-lactide)/poly(ε-caprolactone) blends. Polym J 1997; 29:657–662.
7. Loo YL, Register RA. Crystallization within block copolymer mesophases. In: Hamley IW, editor. Developments in Block Copolymer Science and Technology. Receptor Localization. New York: Wiley; 2004, p 213.
8. Jain RK, Au P, Tam J, Duda DG, Fukumura D. Engineering vascularized tissue. Nat Biotechnol 2005;23:821–823.
9. Puleo DA, Bizios R. Formation of focal contacts by osteoblasts cultured on orthopedic biomaterials. J Biomed Mater Res 1992;26:291–301.
10. Sabino MA, Feijoo JL, Nuñez O, Ajami D. Interaction of fibroblast with poly(*p*-dioxanone) and its degradation products. J Mater Sci 2002;37:35–40.
11. Lim JY, Hansen JC, Siedlecki CA, Hengstebeck RW, Cheng J, Winograd N, Donahue HJ. Osteoblast adhesion on poly(L-lactic acid)/polystyrene demixed thin film blends: Effect of nanotopography, surface chemistry, and wettability biomacromolecules. 2005;6:3319–3327.
12. Takezawa T. A strategy for the development of tissue engineering scaffolds that regulate cell behavior. Biomaterials 2003;24:2267–2275.
13. Kayaman-Apohan N, Karal-Yilmaz O, Baysal K, Baysal BM. Poly(D,L-lactic acid)/triblock PCL-PDMS-PCL copolymers: Synthesis, characterization and demonstration of their cell growth effects in vitro. Polymer 2001;42:4109–4116.
14. Cao Y, Mitchell G, Messina A, Price L, Thompson E, Penington A, Morrison W, O'Connor A, Stevens G, Cooper-White J. The influence of architecture on degradation and tissue ingrowth into three-dimensional poly(lactic-*co*-glycolic acid) scaffolds in vitro and in vivo. Biomaterials 2006;27: 2854–2864.
15. Dell'Erba R, Groeninckx G, Maglio G, Malinconico M, Migliozzi A. Immiscible polymer blends of semicrystalline biocompatible components: Thermal properties and phase morphology analysis of PLLA/PCL blends. Polymer 2001;42: 7831–7840.
16. Hamley IW. The Physics of Block Copolymers. Oxford: Oxford University Press; 1998.
17. Müller AJ, Balsamo V, Arnal ML. Nucleation and crystallization in diblock and triblock copolymers. Adv Polym Sci 2005;190:1–63.

18. Müller AJ, Balsamo V, Arnal ML. Crystallization in block copolymers with more than one crystallizable block. In: Reiter G, Strobl G, editors. Lecture Notes in Physics. Forthcoming.
19. Jacobs C, Dubois PH, Jerome R, Teyssie PH. Macromolecular engineering of polylactones and polylactides. V. Synthesis and characterization of diblock copolymers based on poly-ε-caprolactone and poly(L,L or D,L)lactide by aluminum alkoxides. Macromolecules 1991;24:3027–3034.
20. Hamley W, Castelletto V, Castillo RV, Müller AJ, Martin CM, Pollet E, Dubois PH. Crystallization in poly(L-lactide)-*b*-poly(ε-caprolactone) double crystalline diblock copolymers: A study using x-ray scattering, differential scanning calorimetry, and polarized optical microscopy. Macromolecules 2005; 38:463–472.
21. Hamley IW, Parras P, Castelletto V, Castillo RV, Müller AJ, Mollet E, Dubois PH, Martin CM. Melt structure and its transformation by sequential crystallization of the two blocks within poly(L-lactide)-block-poly(ε-caprolactone) double crystalline diblock copolymers. Macromol Chem Phys 2006;207: 941–953.
22. Sharma PK, Hanumantha Rao K. Analysis of different approaches for evaluation of surface energy of microbial cells by contact angle goniometry. Adv Colloid Interface Sci 2002; 98:341–463.
23. Pei W, Bellows CG, Elsubeihi ES, Heersche JNM. Effect of ovariectomy on dexamethasone- and progesterone-dependent osteoprogenitors in vertebral and femoral rat bone cell populations. Bone 2003;33:822–830.
24. Cei S, Mair B, Kandler B, Gabriele M, Watzek G, Gruber R. Age-related changes of cell outgrowth from rat calvarial and mandibular bone in vitro. J Craniomaxillofac Surg 2006; 34:387–394.
25. Lu HH, Kofron MD, El-Amin SF, Attawia MA, Laurencin CT. In vitro bone formation using muscle-derived cells: A new paradigm for bone tissue engineering using polymer-bone morphogenetic protein matrices. Biochem Biophys Res Comm 2003;305:882–889.
26. Arnal ML, Matos ME, Morales RA, Santana OO, Müller AJ. Evaluation of the fractionated crystallization of dispersed polyolefins in a polystyrene matrix. Macromol Chem Phys 1998;199:2275–2288.
27. Ponsonnet L, Reybier K, Jaffrezic N, Comte V, Lagneau C, Lissac M, Martelet C. Relationship between surface properties (roughness, wettability) of titanium and titanium alloys and cell behaviour. Mater Sci Eng 2003;23:551–560.
28. Magonov SN, Cleveland J, Elings V, Denley D, Whangbo M-H. Tapping-mode atomic force microscopy study of the near-surface composition of a styrene-butadiene-styrene triblock copolymer film. Surf Sci 1997;389:201–211.
29. Reiter G, Castelein G, Sommer J-U, Röttele A, Thurn-Albrecht T. Direct visualization of random crystallization and melting in arrays of nanometer-size polymer crystals. Phys Rev Lett 2001;87:226101/1–226101/4.
30. Knoll A, Magerle R, Krausch G. Tapping mode atomic force microscopy on polymers: Where is the true sample surface? Macromolecules 2001;34:4159–4165.
31. Strobl G. Crystallization and melting of bulk polymers: New observations, conclusions and a thermodynamic scheme. Prog Polym Sci 2006;31:398–442.
32. Salgado AJ, Gomes ME, Chou A, Coutinho OP, Reis L, Hutmacher DW. Preliminary study on the adhesion and proliferation of human osteoblasts on starch-based scaffolds. Mater Sci Eng 2002;20:27–33.
33. Wan Y, Wang Y, Liu Z, Qu X, Han B, Bei J, Wang S. Adhesion and proliferation of OCT-1 osteoblast-like cells on micro- and nano-scale topography structured poly(L-lactide). Biomaterials 2005;26:4453–4459.
34. Gough JE, Christian P, Scotchford CA, Jones IA. Craniofacial osteoblast responses to polycaprolactone produced using a novel boron polymerisation technique and potassium fluoride post-treatment. Biomaterials 2003;24:4905–4912.
35. Safinia L, Datan N, Höhse M, Mantalaris A, Bismarck A. Towards a methodology for the effective surface modification of porous polymer scaffolds. Biomaterials 2005;26:7537–7547.
36. Cooper JA, Lu HH, Ko FK, Freeman JW, Laurencin CT. Fiber-based tissue-engineered scaffold for ligament replacement: Design considerations and in vitro evaluation. Biomaterials 2005;26:1523–1532.
37. Yamato M, Konno CH, Kushida A, Hirose M, Utsumi M, Kikuchi A, Okano T. Release of adsorbed fibronectin from temperature-responsive culture surfaces requires cellular activity. Biomaterials 2000;21:981–986.
38. Teixeira AI, McKie GA, Foley JD, Bertics PJ, Nealey PF, Murphy CJ. The effect of environmental factors on the response of human corneal epithelial cells to nanoscale substrate topography. Biomaterials 2006;27:3945–3954.
39. Tang ZG, Callaghan JT, Hunt JA. The physical properties and response of osteoblasts to solution cast films of PLGA doped polycaprolactone. Biomaterials 2005;26:6618–6624.
40. Lu HH, Tang A, Oh SC, Spalazzi JP, Dionisio K. Compositional effects on the formation of a calcium phosphate layer and the response of osteoblast-like cells on polymer-bioactive glass composites. Biomaterials 2005;26:6323–6334.
41. Dalby MJ, Childs S, Riehle MO, Johnstone HJH, Affrossman S, Curtis ASG. Fibroblast reaction to island topography: Changes in cytoskeleton and morphology with time. Biomaterials 2003;24:927–935.
42. Dalby MJ, Riehle MO, Johnstone HJH, Affrossman S, Curtis ASG. In vitro reaction of endothelial cells to polymer demixed nanotopography. Biomaterials 2002;23:2945–2954.
43. Garcia A, Boettiger D. Integrin-fibronectin interactions at the cell-material interface: Initial integrin binding and signaling. Biomaterials 1999;20:2427–2433.